REPORT DOCUMENTATION PAGE

AFRL-SR-AR-TR-06-0084

1. REPORT DATE (DD-MM-YYYY)	2. REPORT TYPE	3. DATES COVERED (From – To)
October 2005	Final	15 Oct 2002 – 14 Oct 2005

4. TITLE AND SUBTITLE

DEVELOPMENT OF TEXTURED BUFFER LAYER ON METAL TAPES FOR OXIDE SUPERCONDUCTORS

5a. CONTRACT NUMBER

F49620-03-C-0004

5b. GRANT NUMBER

5c. PROGRAM ELEMENT NUMBER

6. AUTHOR(S)

R. S. Bhattacharya and Y. Xu

5d. PROJECT NUMBER

5e. TASK NUMBER

5f. WORK UNIT NUMBER

7. PERFORMING ORGANIZATION NAME(S) AND ADDRESS(ES)

UES, Inc.
4401 Dayton-Xenia Rd
Dayton, Ohio 45432-1894

1. PEFORMING ORGANIZATION REPORT NUMBER

UES P726

9. SPONSORING/MONITORING AGENCY NAME(S) AND ADDRESS(ES)

Air Force Research Laboratory
Air Force Office of Scientific Research
Arlington VA 22203-1954 NE Dr. Harold Weinstock

10. SPONSOR/MONITOR'S ACRONYM(S)

AFOSR/NE

11. SPONSORING/MONITOR'S REPORT NUMBER(S)

12. DISTRIBUTION/AVAILABILITY STATEMENT

Approved for public release; distribution is unlimited

13. SUPPLEMENTARY NOTES

14. ABSTRACT

Report documents the development effort dedicated to the scale up of inclined substrate deposition (ISD) of textured magnesium oxide (MgO) on continuous tapes of nickel based alloys under an AFOSR Phase II STTR program, in partnership with Argonne National Laboratory (ANL). Long length highly textured MgO template has been successfully deposited on HC substrate in the reel-to-reel system. High deposition rate up to 10 nm/sec of the ISD MgO ebeam deposition and broad exposure window of 7 cm have been achieved with the average in-plane texture of FWHM=10°. With this set up the output of the well textured MgO template can be easily reached to 1 m/hr. Texture formation of the MgO layer has been investigated by XRD analysis. A new relationship termed "two-third relationship"between inclined angle and the tilted angle of (00l) plane is found for the present experimental set up. YBCO-coated conductors fabricated on lightly polished Hastelloy C (HC) substrate with the ISD-MgO capped with Strontium Ruthenate (SRO) buffer layer exhibited a sharp transition with Tc = 90 K. Transport $Jc = 0.68\times10^6$ A/cm^2 and Ic > 44 A/cm were measured at 77 K in self-field. Using highly polished HC surface, J_c increased to over 1.6 $\times10^6$ A/cm^2 and I_c increased to 110 A/cm.

15. SUBJECT TERMS

Inclined Substrate Deposition, ISD MgO, High Temperature Superconductor, Coated Conductor, Textured Buffer Layer, Yttrium Barium Copper Oxide

16. SECURITY CLASSIFICATION OF:			17. LIMITATION OF ABSTRACT	18. NUMBER OF PAGES	19a. NAME OF RESPONSIBLE PERSON
a. REPORT	b. ABSTRACT	c. THIS PAGE			Dr. Harold Weinstock
Unclassified	Unclassified	Unclassified	SAR	22	19b. TELEPHONE NUMBER (Include area code) 703-696-8572

TABLE OF CONTENTS

SECTION		PAGE
ILLUSTRATIONS		iii
FOREWARD		iv
1.0	INTRODUCTION	1
2.0	OBJECTIVES	1
3.0	EXPERIMENTAL PROCEDURE	2
4.0	EXPERIMENTAL RESULTS AND DISCUSSION	3
4.1	Texture Development	3
4.2	Long Length Tape	8
4.3	Microstructure and Surface Morphology	10
4.4	YBCO and ISD MgO	12
4.5	MOD of YBCO	14
5.0	SUMMARY	15
REFERENCES		15

ILLUSTRATIONS

SECTION **PAGE**

Figure 1 (a) Schematic diagram showing the principle of electron beam evaporation and inclined substrate deposition system. α is the inclined angle of substrate and β is the tilt angle of the MgO (001) plane from the substrate normal. (b) The reel to reel deposition system equipped with a high power electron gun, two cylindrical sputter coaters and one linear sputter coater.... 2
Figure 2 Pole figure analysis of ISD MgO deposited at 25°, 30°, and 35°, respectively.... 4
Figure 3 (002) Pole figure analysis of ISD MgO deposited at 40°, 55°, and 57°, respectively.... 5
Figure 4 Phi scans of MgO template deposited at 35° and 55°, respectively.... 5
Figure 5 XRD θ-2θ scans of ISD MgO deposited at 35° and 55°, respectively.... 5
Figure 6 Thickness dependence of the in-plane texture formation of ISD MgO deposited at 35°, and 55°, respectively. The inset also shows a simulation of the layer by layer evolution of MgO in-plane texture.... 6
Figure 7 A comparison of the tilted angles predicted by different laws with measured values.... 8
Figure 8 Position dependence of the MgO in-plane texture for a meter long tape.... 9
Figure 9 Position dependence of the MgO in-plane texture for the 7 cm exposure window.... 9
Figure 10 MgO in-plane texture for a meter long tape.... 9
Figure 11 Surface morphology of the ISD MgO template deposited at different inclined angles.... 10
Figure 12 (a) Cross sectional TEM shows the columnar structure. The inset is the SAD pattern showing the texture development. (b) TEM surface morphology of the ISD MgO template deposited at α=35. (c) AFM surface morphology of the ISD MgO template deposited at α=55.... 11
Figure 13 Schematic drawings showing (a) the orientation relationship of MgO unit cell with Respect to substrate and oblique flux. (b) Truncated {002} planes observed from the substrate normal. (c) Truncated {002} planes observed from MgO flux direction.... 12
Figure 14 Pole figure analysis on MgO (002), YBCO (005), (103), and (113), respectively.... 12
Figure 15 T_c and I_c measurement of the YBCO film deposited on ISD MgO with SRO cap layer.... 13
Figure 16 SIMS analysis of the YBCO film deposited on ISD MgO with SRO cap layer.... 13
Figure 17 AFM surface analysis of the ISD MgO template deposited on (a) lightly mechanical polished HC tape and (b) well polished small HC sample.... 14
Figure 18 I_c measurement of YBCO film on highly polished HC surface with ISD MgO template and SRO buffer layers.... 14

Table 1 Relationship of inclined angle and measured tilted angles as well as value predicted by popular formulas.... 7
Table 2 AFM surface statistics of ISD MgO template deposited on lightly mechanical polished HC tape and well polished small HC sample.... 14

FOREWARD

This work was performed by UES, Inc. in cooperation with the subcontractor, Argonne National Laboratory (ANL). This report presents the results of SBIR Phase II from AFOSR, Contract No. F49620-03-C-0004, performance period October 15, 2002 – October 14, 2005. The AFOSR technical point of contact is Dr. Harold Weinstock. The Principal Investigator of this work is Dr. Rabi Bhattacharya. The report is co-authored by Dr. Y. Xu, who has performed many of the technical tasks. The subcontract effort is led by Dr. U. (Balu) Balachandran. Dr. B. Ma of ANL has provided excellent technical support. The contributing efforts of Mr. M. Massey, Mr. H. Evans and Ms. Jan Clark of UES in performing various tasks are gratefully acknowledged.

FINAL REPORT

October 15, 2002- October 14, 2005

DEVELOPMENT OF TEXTURED BUFFER LAYER ON METAL TAPES FOR OXIDE SUPERCONDUCTORS

STTR PHASE II
CONTRACT NO. F49620-03-C-0004
CONTRACT TYPE:CPFF PHASE II AMOUNT: $499,980

SUBMITTED TO

Dr. Harold Weinstock
4105 Wilson Blvd., STE. 713
Arlington, VA 22203 – 1977

SUBMITTED BY

UES, Inc.
4401 Dayton-Xenia Road
Dayton, OH 45432
(937) 426-6900

PRINCIPAL INVESTIGATORS

Dr. Rabi S. Bhattacharya
Dr. Y. Xu
UES Materials Laboratory

SUBCONTRACTOR

Argonne National Laboratory
Dr. U. (Balu) Balachandran
Dr. B. Ma

1.0 INTRODUCTION

Second generation (2G) coated conductor (CC) wire based on $YBa_2Cu_3O_{7-x}$ (YBCO or Y123) and other $ReBa_2Cu_3O_{7-x}$ (ReBCO, Re rear earth) have attracted extensive interest in recent years because of their potential applications in the electric power industry including cable, motor, generator, transformer etc. [1-5]. YBCO needs to be biaxially aligned otherwise weak links at high-angle grain boundaries in the film limits the ability of carrying high current [6]. Great efforts have been expended onto the texture formation of YBCO films and robust techniques for developing textured YBCO on flexible metallic substrates have been realized through RABiTS (rolling assisted biaxial textured substrates) [7, 8], IBAD (ion beam assisted deposition)[9-12], and ISD (inclined substrate deposition)[13-15]. IBAD method was initially developed by Harper et al at 1984[16], further by Rassnagel et al in 1987[17], and then introduced to the growth of textured YSZ buffer for YBCO films by Iijima in 1991[10]. While by using inclined substrate deposition (ISD) without the assistance of the ion beam, Fujino and Hasegawa [13] made the textured YSZ template on Ni-based alloy by PLD. Later on, in 1998, Bauer et al. [14] used the similar idea and grew MgO buffer successfully on Hastelloy C276 by evaporation method. The research that followed on ISD MgO is very successful in Europe [18], Japan [19] and the United States [20].

The idea of inclined substrate deposition can be traced long time back to 1959 termed oblique evaporation/deposition. The discovery by Smith was made during the evaporation of permalloy on rather large substrates [21, 22]. The research on the oblique evaporation has been very active since then especially for the fabrication of thin films with anisotropic magnetic properties [23]. The advantage of the ISD deposition is that high deposition rate up to 10 nm/sec can be used which is suitable for the long length tape deposition. Texture of ISD MgO evolves rapidly at room temperature for films of 1-3 μm thick on nontextured metal substrates. Many efforts have been focused on understanding the mechanism of texture formation in an ISD/oblique deposition. It is commonly accepted that the texture develops by an evolutionary shadowing process where only textured columns survive [24]. Much effort has been expended on ISD MgO in Europe. In the past five years, the in-plane texture of ISD MgO has been much improved from about 20° of FWHM in the phi scan to below 10°. As a result, the critical current density, J_c, increased to 2.5 MA/cm^2 and I_c >400A/cm has been demonstrated [25]. Recently, buffered tape has been fabricated up to 40 m length. The subsequent HTS deposition has been performed up to 12 m and reached current levels of 200 A/cm [25]. In the United States, Argonne National Laboratory has been leading the research in ISD since 2001 [26]. UES has been working with ANL for the past few years funded by the AFOSR Phase II STTR program. This report describes the details of the scale-up effort of ISD MgO buffer layer deposition at UES and constitutes the final report of the project.

2.0 OBJECTIVES

This Phase II STTR program was in partnership with Argonne National Laboratory (ANL). The overall objective of the Phase II program was to scale up the process of deposition of textured MgO on continuous tapes of nickel based alloys using inclined substrate deposition (ISD). UES has a reel-to-reel sputter system for continuous coating of long wires or tapes. A major objective in Phase II was to modify the existing reel-to-reel magnetron sputter coating system for continuous coating of polycrystalline metal alloy tapes using e-beam evaporation. UES proposed to optimize the deposition process for ISD MgO-based buffer architecture using this reel-to-reel system for long length deposition of textured MgO. Although, ANL has recently demonstrated that by optimizing the layer thicknesses and deposition conditions of various layers in the multilayer architecture of ISD MgO, they could achieve J_c over 1 MA/cm^2 on short samples, it has not been accomplished on a long tape [26]. A number of steps are involved in this process: (1) deposition of an YSZ layer by magnetron sputtering, (2) ISD of MgO, (3) epitaxial MgO at substrate temperature >700C, (4) epitaxial YSZ layer at substrate temperature >700C, (5) epitaxial CeO_2 at substrate temperature >700C (Figure 2). All these depositions have to be done on a moving tape at a steady deposition rate for uniform thickness. The steps 4 and 5 can be combined with a

single layer deposition of strontium ruthenate (SRO) [26]. Thus, the goal of the project was to optimize the deposition conditions for a moving tape to obtain similar results as on the static tape thereby enabling long length buffered tape development for coated conductor.

3.0 EXPERIMENTAL PROCEDURE

The MgO template layer was deposited by ISD with electron beam evaporation at room temperature from fused lumps of MgO target material. Figure 1 (a) and (b) shows the schematic diagram of principle of the e-beam ISD deposition and the reel to reel deposition system. The R2R system is equipped with high power e-gun and three sputtering guns: two cylindrical and one linear sputter guns. Pumps of mechanical, turbo, and cryogenic are attached to the system with the capability to bring the pressure down to the 10^{-7} Torr. All buffer layers can be put down in the same system without breaking the vacuum. Tape is driven by stepper motor with a very broad moving speed from few centimeters/hr to tens of meters/hr. Four two-inch-diameter crucibles can hold more than 400g MgO target material, which is good for MgO deposition on a few 100 meter tapes. Metal tape substrate is mounted on or attached to a tiltable sample stage above the e-beam evaporation source. The inclined angle of sample stage is adjustable to a precision of 0.5°. The temperature of sample stage is monitored with K type thermocouple by attaching it to the stage. Oxygen flow was introduced into the system during deposition at a rate of 5 ml/min which results in a pressure increase in the chamber to 10^{-5} Torr range. A quartz crystal monitor was mounted near the substrate to measure the deposition rate and control film thickness. Typical thickness of the ISD MgO layer is 2 to 3 μm in this research under the deposition rate of 2-10 nm/sec. A series of inclined angles were investigated for texture development and surface roughness. Based on previous results and other reports [25, 27] our research focused, in particular, on α=35° and 55°, where the substrate inclination angle α is defined as the angle of substrate normal with respect to the evaporation direction.

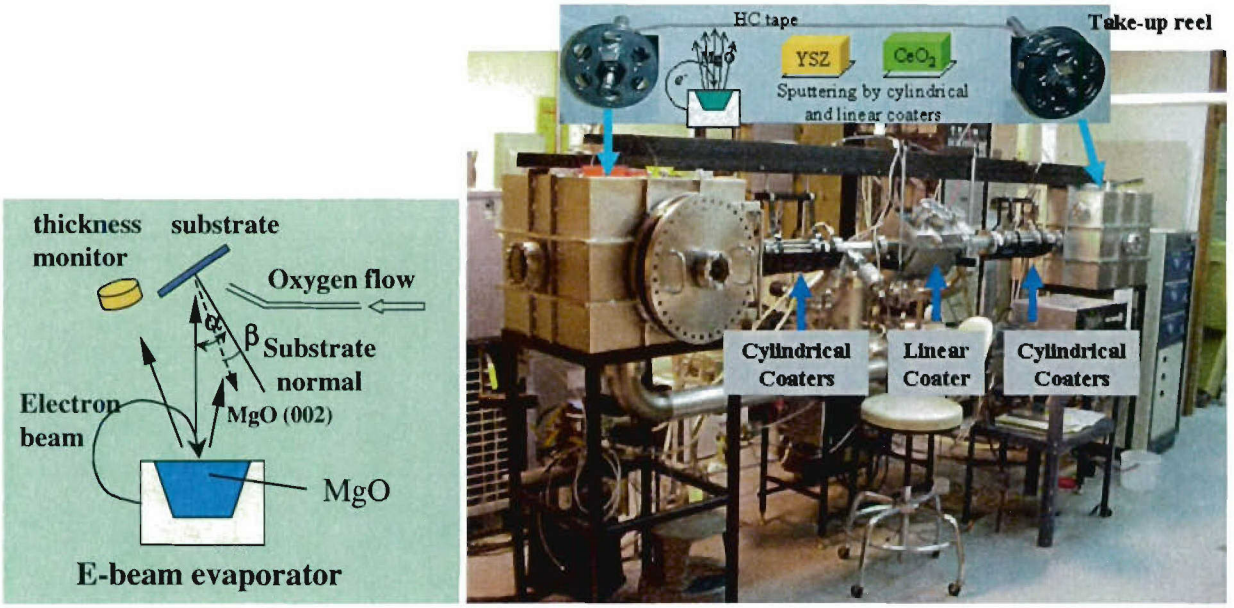

Figure 1. (a) Schematic diagram showing the principle of electron beam evaporation and inclined substrate deposition system. α is the inclined angle of substrate and β is the tilt angle of the MgO (001) plane from the substrate normal. (b) The reel to reel deposition system equipped with a high power electron gun, two cylindrical sputter coaters and one linear sputter coater.

A homo-epitaxial MgO layer of 300 nm was grown on the ISD MgO at 725°C and zero degree inclination angle to improve the surface quality. Compared with ISD MgO, the addition of homo-epitaxial MgO produces dense and smooth surface layer with improvement in the in-plane texture by 2-4 degrees. SRO and YBCO films were deposited on ISD-MgO substrates using a Lambda Physik LPX 210i excimer laser, with a Kr-F_2 gas premixture as the lasing medium. This device generates a pulsed laser beam of 248-nm wavelength and 25-ns pulse width. The SRO and YBCO targets were 45 mm in diameter and 6 mm thick. The ISD-MgO substrates were attached to a heatable sample stage with silver paste and heated to an elevated temperature (700 - 800°C) during deposition. The size of the laser spot focused at the rotating target was 12 mm^2, which produced an energy density of 2.0 J/cm^2. The distance between the target and the substrates is about 7 cm. During deposition, oxygen partial pressure, which was obtained by flowing ultrahigh-purity oxygen through the vacuum chamber, was 50 mTorr for the SRO buffer and 200 mTorr for the YBCO film.

The substrate tape used for this research is Ni-based polycrystalline Hastelloy C-276 (HC) from Goodfellow. The use of HC as substrate material is because of its desirable mechanical strength, compatible thermal properties, and in particular, its nonmagnetic properties. The tape is quarter inch wide and about 150 microns thick. Light mechanical polishing was applied followed by a standard cleaning process before the deposition of oxide layers. Few small samples with very well polished surface were also prepared for comparison purpose. The films used for TEM analysis were deposited on amorphous YSZ buffered Si single crystal.

X-ray diffraction (XRD) θ-2θ scans were used for the phase examination and texture analysis. XRD phi-scan measurements were used to evaluate in-plane texture in terms of full width at half maximum (FWHM). Statistical distribution of oriented grains characterized by XRD Pole figure analysis was performed on the four-circle X-ray diffractometer. Surface morphology was examined by optical microscopy, scanning electron microscopy (SEM), and atomic force microscopy (AFM). Cross sectional structure, composition, and grain orientation were examined with transmission electron microscopy (TEM), energy dispersive spectroscopy (EDS), and selected area diffraction (SAD). Also film thickness was observed in the TEM analysis. YBCO critical transition temperature (T_c) was determined by an inductive method and, transport J_c was measured by the standard four-probe method at 77 K self-field using a 1 μV/cm criterion.

4.0 EXPERIMENTAL RESULTS AND DISCUSSIONS

4.1 TEXTURE DEVELOPMENT

The 2G coated conductors are fabricated on flexible metal tape by the epitaxial growth of ReBCO on textured buffer layers. Thus, the texture quality of the buffer layer is critical for the electrical performance of the YBCO films. Based on the experimental results on bi-crystal reported by Dimos et al [6], for the YBCO superconductor, the mis-orientation at a grain boundary is the source of weak link. Hence, reducing the mis-orientation angles and improving the texture of buffer layers are critical for the electrical performance of YBCO films. To investigate the texture development, we systematically studied the factors that may have impact on the orientation of MgO grains. Figure 2 shows the pole figures in linear scale of the MgO (002) and MgO (111) planes on the ISD MgO templates deposited under 25°, 30° and 35° of the inclined angles, respectively. In this case the thickness of MgO layer is 1.5 μm. First of all, the off center pattern with the unsymmetrical poles of MgO (002) plane indicates that the c-axis of MgO unit cell tilts from substrate normal. The tilted angles (β) of the (001) plane were measured from the χ-angle of the strongest peak and listed in Table 1. These pole figures also tell the information of the texture evolution. Apparently, under these deposition angles, all of the ISD MgO templates show the out-of-plane texture. The equiaxed (200) poles for all of the three pole figures reveal that the columnar structure has

developed from the very begining, otherwise the pole expands and the ratio of the pole's dimension along r and θ direction should be off greatly from 1. The smaller size of the pole on the MgO deposited at α=35° indicates that the out-of-plane texture evolves faster with the increase of inclined angle. However, the development of in-plane texture is quite different, as shown in Figure 2, for the small inclined angle of $\alpha \leq 30°$. The pole figure of the MgO (111) plane shows limited grain alignment for α=25° and 30°, respectively. Though much improvement has been observed for α = 35° (Figure 2), the high aspect ratio of pole in r and θ directions indicates that the development of in-plane texture is sluggish and grain alignment along this direction is broad. As the pole figure is the statistical result of the whole MgO layer, the broad orientation is mainly from the bottom part and the top layer is much improved. The good texture of SRO grown on top of MgO is the direct evidence of this effect [26].

For the high angle depositions, the texture development is faster compared with those deposited at lower deposition angles. With the increase of the inclined angle, the tilted angle β of MgO (00l) plane from the substrate normal increases and three poles can be observed on the pole figure. Figure 3 shows the pole figures in square root scale taken on MgO (002) plane deposited under different inclined angle of 40°, 55° and 57° which yield the pole intensities of 19993, 33525, and 19126 counts respectively. We can see the texture improvement especially for the α=55°. To compare the in-plane texture directly, phi scans of MgO (002) plane were performed on α=35° and 55° for 2.5 μm ISD MgO, and the data were plotted in Figure 4. For this 2.5μm ISD MgO, the in-plane texture of FWHM has been found to be below 10° for the α=55° deposition. However for the deposition of α=35°, FWHM value is 15°, much higher compared with that deposited at α=55°. Another big difference observed is the phi scan intensity; the counts for α=55° is about four times the value of α=35°. Also the background for the α=35° deposition is higher, which means broad oriented grains. To check the existence of polycrystalline grains, XRD θ-2θ scans were performed on these two samples and the reflection peaks are shown in Figure 5. The small peaks of MgO (111) and (220) observed on the XRD θ-2θ scan for the ISD MgO deposited at α=35° confirmed the existence of random oriented grains. However, the XRD θ-2θ scan does not show (111) and (220) peaks even using log scale for the MgO film deposited at α=55°, which indicates that the MgO grains are very well aligned. All of these experiments confirm that the texture of ISD MgO develops faster for the high inclined deposition angle.

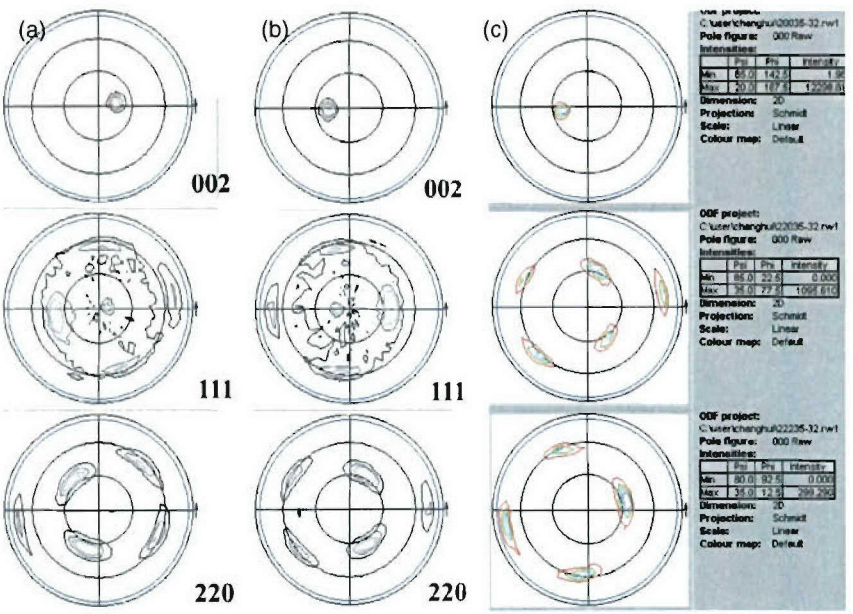

Figure 2. Pole figure analysis of ISD MgO deposited at 25°, 30°, and 35°, respectively.

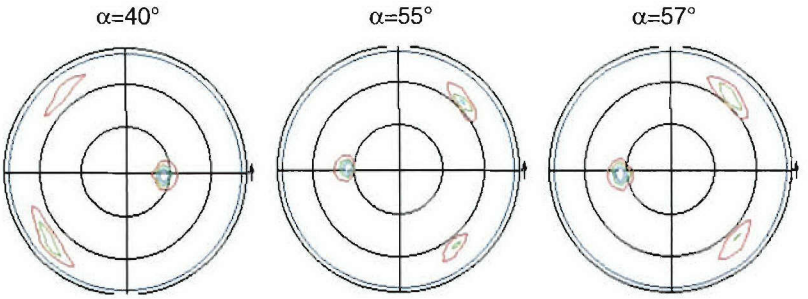

Figure 3. (002) Pole figure analysis of ISD MgO deposited at 40°, 55°, and 57°, respectively.

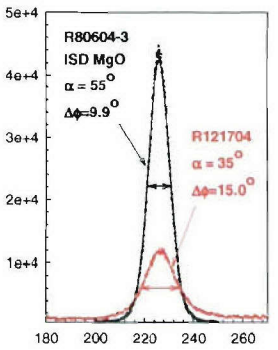

Figure 4. Phi scans of MgO template deposited at 35° and 55°, respectively.

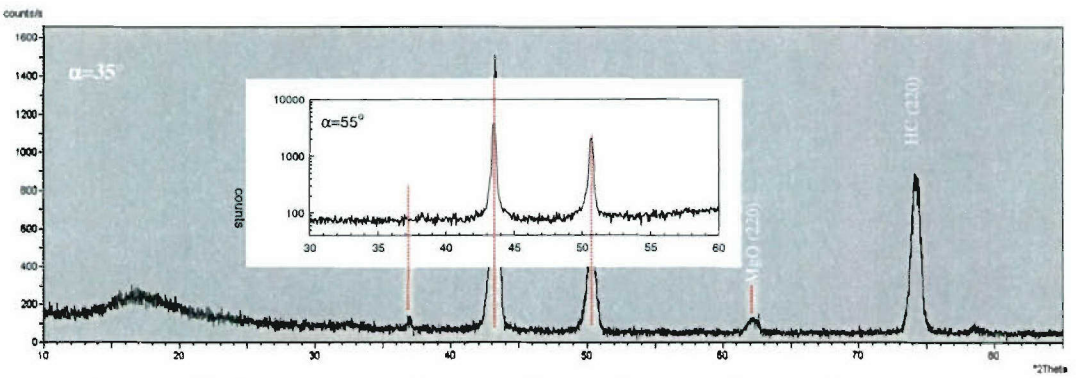

Figure 5. XRD θ-2θ scans of ISD MgO deposited at 35° and 55°, respectively.

Figure 6 is the Gaussian fits to the orientation distribution of in-plane texture, and the insert shows the thickness dependence of the ISD MgO in-plane texture for the deposition at inclined angles of α=35° and 55° respectively. By fitting the experimental data, the texture evolution based on FWHM of MgO (002) plane for α=35° and 55° can be given in the following formulas:

$$\Delta\Phi = 5.1008x^4 - 28.644x^3 + 62.719x^2 - 68.939x + 46.431 \quad (1)$$

$$\Delta\Phi = -4.5745x^3 + 25.595x^2 - 47.084x + 39.954 \quad (2)$$

where, $\Delta\Phi$ is the value of FWHM, and x is the film thickness.

Through these formulae we can see that the in-plane texture is correlated to the power four of the thickness for the MgO film deposited at inclined angle of α=55°, while, for α=35°, the power is three, which means the convergence of the former is faster with thickness than the later, that is the texture evolves quickly for the higher inclined angle depositions.

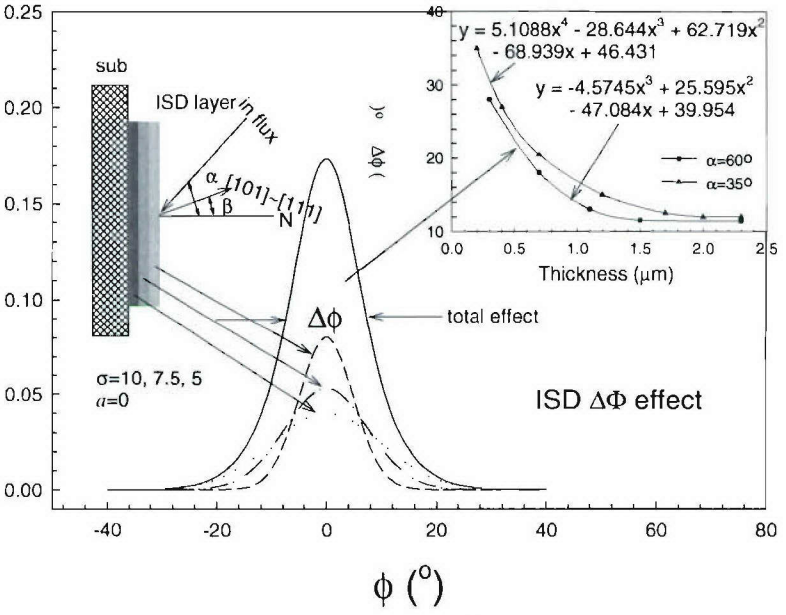

Figure 6. Thickness dependence of the in-plane texture formation of ISD MgO deposited at 35°, and 55°, respectively. The inset also shows a simulation of the layer by layer evolution of MgO in-plane texture.

Many factors play role on the texture development of ISD MgO template. Under an oblique deposition, anisotropic growth rate and limited atomic diffusion are the decisive factors. Their combination determines the rate of texture evolution. Apparently, appropriate temperature, which represents the kinetic energy of atoms, is very important for the texture development. As described above, the root cause for the texture formation in the oblique deposition is the shadowing effect, and the following "tangent law" has been proposed for the growth [28,29]:

$$\tan\beta = \frac{1}{2}\tan\alpha \qquad (3)$$

This empirical relationship indicates that shadowing is the governing mechanism in the oblique deposition. Based on geometrical arguments, Tait et al. derived another expression relating β to α for the case of limited surface diffusion,

$$\beta = \alpha - \sin^{-1}\left[\frac{1-\cos\alpha}{2}\right] \qquad (4)$$

We have performed inclined depositions from α=25° to α=57°. Table 1 shows the relationship of the measured tilted angle β with inclined angle α as well as the predicted values from "TAN law" and Tait's formula. Based on the measured values, we propose a new formula termed "two-third relationship" by fitting these data:

$$\beta = \tfrac{2}{3} \cdot \alpha' - 1.3 \qquad (5)$$

Based on this linear "two-third relationship", β values can be predicted with the least errors to the experimental data. As a comparison, Figure 7 shows all data including those predicted by "TAN law" and Tait's formula.

As of the nature of the ebeam deposition, the hitting spot of the electron beam may shift from the geometric center of the crucible containing MgO target materials; for example a 3- 4 mm shift is small compared to the crucible of ϕ=51 mm, but it may introduce a system error of 1.7- 2.3° for the inclined angle. So a new formula can be derived:

$$\begin{aligned} \beta &= \tfrac{2}{3} \cdot \alpha' - 1.3 \\ &= \tfrac{2}{3}(\alpha' - 1.95) \\ &= \tfrac{2}{3} \cdot \alpha \end{aligned} \qquad (6)$$

where, α is the true value of the inclined angle.

Formula (6) gives a new relation between inclined angle α and the tilted angle β. We have not determined the mechanism for the "two-third relationship"; as a mater of fact, this formula predicts the β values much closer to the measured ones compared to all other empirical or theoretical relationships [32, 34, 35]. The "two-third relationship" needs to be tested in different deposition systems.

Table 1. Relationship of inclined angle and measured tilted angles as well as value predicted by popular formulas

α (°)	25	30	35	40	45	50	53	55	57
Measured β_0 (°)	15.27	18.26	21.66	25.21	29.28	31.30	33.46	35.53	35.91
β_1=2α/3-1.3	15.37	18.70	22.03	25.37	28.7	32.03	34.03	35.37	36.7
$\beta_1 - \beta_0$ (°)	0.10	0.44	0.37	0.16	-0.58	0.73	0.57	-0.16	0.79
TAN law β_2 (°)	13.12	16.10	19.30	22.76	26.56	30.79	33.56	35.53	37.59
$\beta_2 - \beta_0$ (°)	-2.15	-2.16	-2.36	-2.45	-2.72	-0.51	-0.1	0	1.68
Tait formula, β_3 (°)	22.31	26.16	29.81	33.28	36.58	39.71	41.52	42.69	43.84
$\beta_3 - \beta_0$ (°)	7.04	7.90	8.15	8.07	7.30	8.41	8.06	7.16	7.93
β=2α/3	16.67	20.00	23.33	26.67	30.00	33.33	35.33	36.67	38

Note: $\sum_{25}^{53}(\beta_1 - \beta_0)^2 = 2.21$, $\sum_{25}^{53}(\beta_2 - \beta_0)^2 = 31.35$, $\sum_{25}^{53}(\beta_3 - \beta_0)^2 = 546.65$

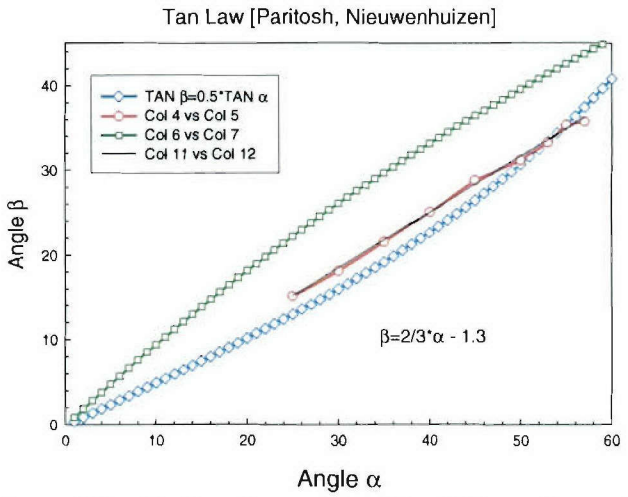

Figure 7. A comparison of the tilted angles predicted by different laws with measured values.

4.2 LONG LENGTH TAPE

High deposition rate up to 10 nm/sec of the ISD ebeam deposition is one of the advantages for the texture formation over other approaches. While to scale up, we need not only the high deposition rate but also the deposition area, because the amount of material delivered is the product of the deposition rate and deposition surface area. For a given thickness, the output of coated tape is proportional to this product. In our system, except for the high rate deposition, we have extended the deposition from the small "sweet spot" (≈ 1 cm) to an exposure length of 7 cm, which makes a yield of 1 meter/hr for the deposition rate of 10 nm/sec. As of the broadening of the flux plume, it is usually believed that the texture degrades with the extended exposure area. Geometrically for the 7 cm exposure window, it gives the aspect ratio of 7cm/1cm=7. So, two inclination module can be applied. Initially the deposition is performed on an orientation (orientation I) with TD (transverse direction) leveled but the RD (rolling direction) inclined 55°; the combination of divergence of the flux plum and height different resulted in a relative broad in-plane texture. Another disadvantage is the direction of dense MgO is along the TD with loose MgO on the RD direction. The position dependence of the in-plane texture is shown in Figure 8. It is well known that inclination leads to an anisotropic electrical and magnetic properties. Usually, critical current in the tilted direction is lower compared to the untilted direction. The ratio between the high J_c value perpendicular and the low J_c parallel to the tilt direction can range up to a factor of two[14]. To improve the electrical properties and take the advantage of the texture orientation, the deposition is then reconstructed to an orientation (orientation II) with RD leveled but the TD inclined 55°. The grain alignment under this orientation is much improved compared to orientation I. For the 7 cm HC tape, the in-plane texture is carefully characterized and the position dependence of MgO (002) in-plane texture is shown in Figure 9. This 7 cm tape shows good in-plane texture especially for the center five sections, each of which has $\Delta\Phi$ below 10°. The $\Delta\Phi$ value increases about 2° for both end and reach the value of 11.3 - 11.4°. The overall average value of $\Delta\Phi$ comes to 10.0°, but if we count only the center five sections, they have an average of 9.5°. That means by adjusting the exposure window, in-plane texture could be further improved. With this orientation, long length continuous deposition in our reel-to-reel system have been deposited and the check point of in-plane texture is schematically shown in Figure 10.

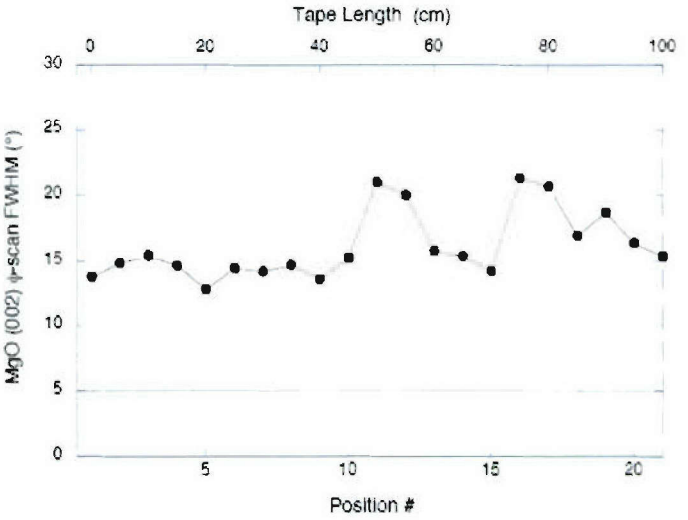

Figure 8. Position dependence of the MgO in-plane texture for a meter long tape.

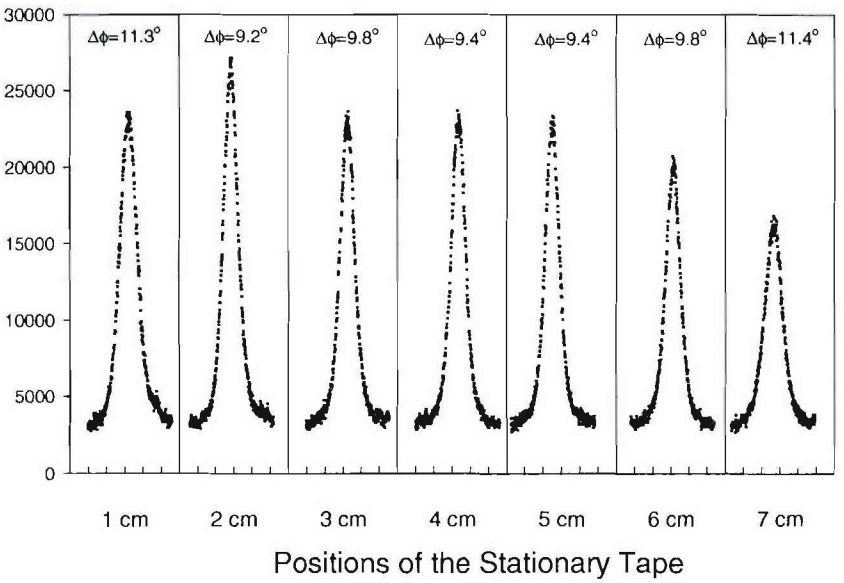

Figure 9. Position dependence of the MgO in-plane texture for the 7 cm exposure window.

Figure 10. MgO in-plane texture for a meter long tape.

4.3 MICROSTRUCTURE AND SURFACE MORPHOLOGY

Figure 11 is the SEM surface morphology of the ISD MgO films deposited under different angles of 25°, 30°, 35°, 50°, 55°, and 57°. Roof tile structure has been shown on all films deposited in the broad angle from 25° to 57°, indicating the formation of the columnar structure with in-plane and out-of-plane texture. However, surface morphology changes dramatically with the increase of the inclined angle α. The SEM picture shows that the distance between the tile front of adjacent layers decreases with the increase of the angle α. This distance change reflects the β angle change and keeps the same trend as shown in Figure 7. Voids start to appear at deposition angle of 35° and very loose structure is commonly observed at high inclined angle especially for $\alpha > 50°$. As a result, the surface becomes rough for high angle deposition. Orientation analysis in the previous section has shown that texture evolves faster with inclined angle; this obviously is a trade-off with the surface smoothness.

Increasing the inclination angle significantly improves the in-plane texture of the films. This improvement is demonstrated in the SAD pattern in Figure 12 (a), which corresponds to a cross-sectional TEM image of MgO deposited at $\alpha = 55°$. SAD patterns from various regions throughout the thickness are also shown and clearly indicate an improvement in texture as the film grows. The pattern from the region immediately above the interface demonstrates polycrystalline orientation. The film becomes well-textured at a thickness of about 1μm. Figure 12 (a) also shows the variation in columnar morphology of grains as the film grows. A thin and dense fiber grains of about 20 nm is shown for the initial depositions. On the upper portion of a 3 μm film, on the other hand, columnar grains are thicker (=100-200 nm) and exhibit cubic morphology.

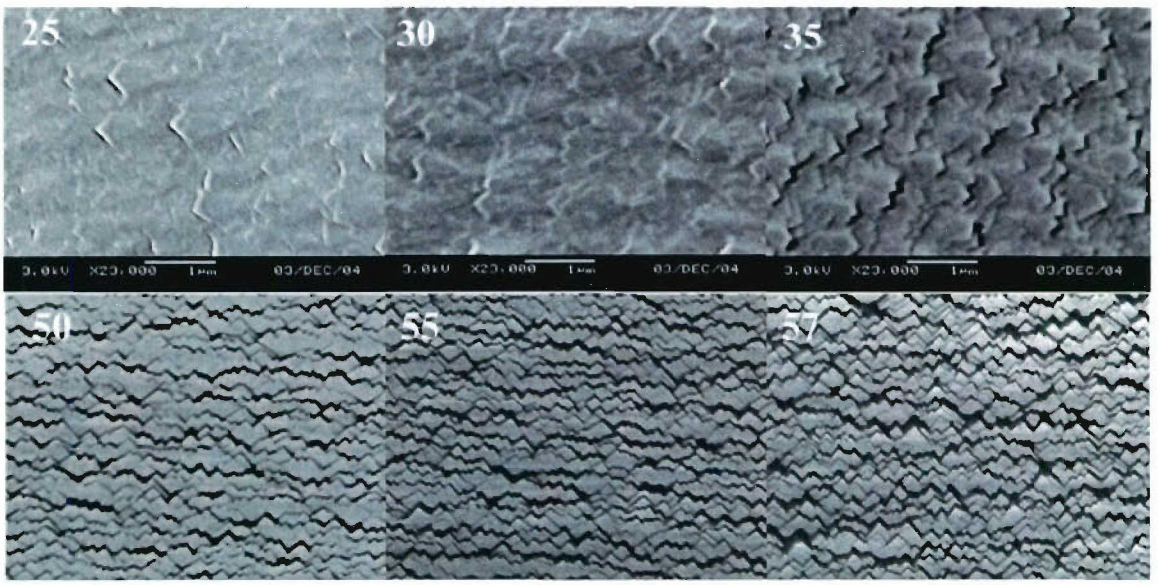

Figure 11. Surface morphology of the ISD MgO template deposited at different inclined angles.

In all growth conditions in this study and by others [14, 36, 37], the (002) plane rotates to face the vapor flux and not the (111) face as deposited at $\alpha = 0°$. That is, the [111] direction rotates to grow away from the vapor when the substrate is inclined. This is further confirmed by the plan view TEM analysis as shown in Figure 12 (b). The TEM photomicrographs of the MgO thin films grown by ISD clearly show that the MgO crystal habit is in fact cubic with (002) as the tile surface plane confirmed by SAD pattern. This observation suggests that, in the competition of (002) and (111) growth, the MgO crystals prefer to

grow with the [11n] direction perpendicular to the substrate while maintaining a minimization of surface free energy by maximizing the (200) surface area at off substrate normal.

Maximization of the (200) surface area per unit volume while maintaining the required [111] preferred growth direction perpendicular to the substrate is obtained by growing as pyramids. Accordingly, the higher packing density in this direction and the lowering of surface free energy drive the formation of (002) crystal faces that grow at an angle to the substrate normal.

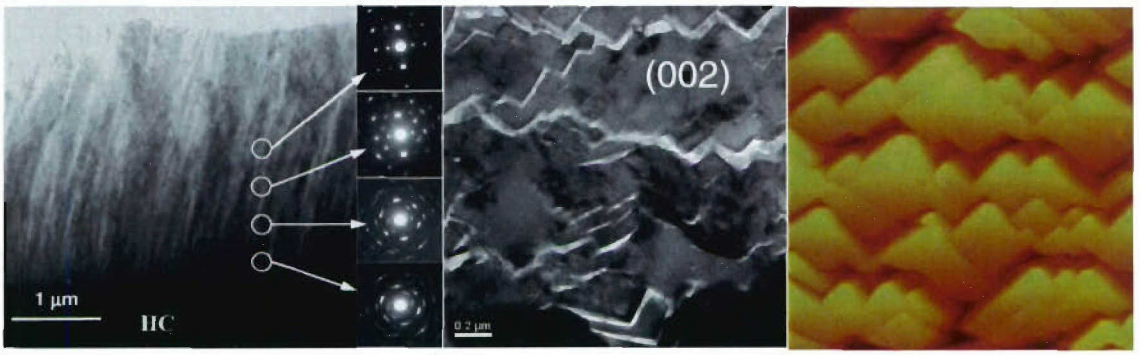

Figure 12. (a) Cross sectional TEM shows the columnar structure. The inset is the SAD pattern showing the texture development. (b) TEM surface morphology of the ISD MgO template deposited at α=35. (c) AFM surface morphology of the ISD MgO template deposited at α=55.

As flux of the vapor is oblique with respect to the substrate normal, the fast outgrowth of highly packed plane prevails and takes over the growth trend by shadowing grains with other orientations. Most commonly it was believed that the MgO (111) plane was the preferred growth direction, however, as a matter of fact, in all of our experiments it is shown that [111] turns slightly off the substrate normal. Depending on the inclined angle α, the crystal orientation indexed [11n], between [111] and [113] of MgO, grows parallel to substrate normal. The requirement of reducing surface energy while maintaining the [11n] preferred growth direction has truncated MgO columnar growth with {100} faces, one of which is rotated to face the vapor direction. In a real growth process, the cross section of the deposition flux must be taken into account. Experimental result indicates that {100} plane has the greatest capture cross section, and it turns towards the MgO vapor direction by outgrowth of grains with preferred orientation. Accordingly, in the oblique or ISD deposition, the in-plane texture is defined by the preferred growth direction of [11n]//substrate normal and one of the {100} planes rotates to the in-flux direction. This defined orientation is represented by the following relationship and shown in Figure 13 (a).

$$\left.\begin{array}{ll} & [11n]//\mathbf{N} \\ \text{and} & [001]\rightarrow \mathbf{J} \end{array}\right\} \qquad (7)$$

As long as the difference between **N** and **J** directions is large enough, the preferred growth can be sustained and texture will be achieved. That is, given an α larger than a specific angle, for example α>20°, MgO in-plane texture can be formed, otherwise the growth of oriented grains collapses and in-plane texture loses its track. Figure 13 (b) is a schematic drawing showing the facet of the textured MgO top surface observed from the **N** and **J** directions, respectively. Following the commonly observed rule of crystal growth, the preferred growth direction only happens to a highly packed plane of MgO which defines n in between 1 and 3. So once α is smaller than some value, [11n] can not keep up with the substrate normal **N**, and preferred growth can not be sustained. In this case out-of-plane texture may be observed because of the columnar growth, but in-plane texture is not expected,

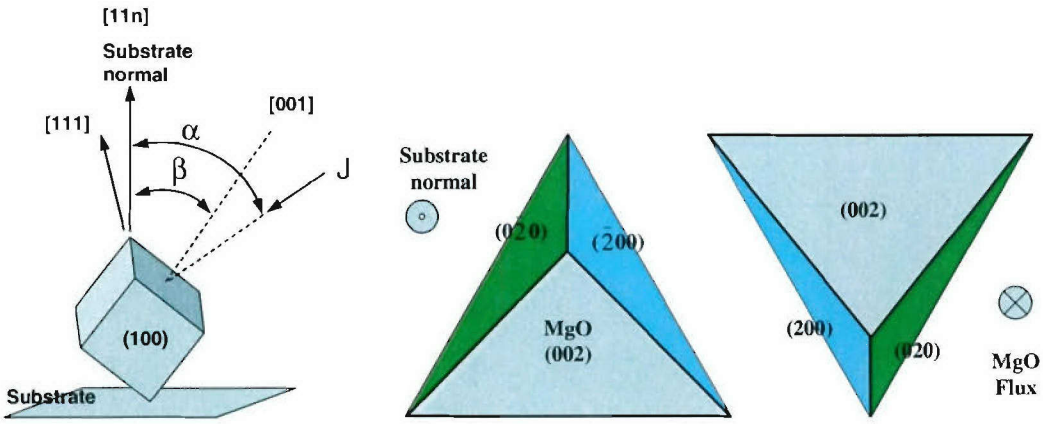

Figure 13. Schematic drawings showing (a) the orientation relationship of MgO unit cell with respect to substrate and oblique flux. (b) Truncated {002} planes observed from the substrate normal. (c) Truncated {002} planes observed from MgO flux direction.

4.4 YBCO ON ISD MgO

The MgO template used for the YBCO deposition was grown at an inclined angle of 55°. Before YBCO growth, a 200 nm homo-epitaxial MgO layer was grown on the ISD MgO at 725°C to smooth out the surface, followed by a 200 nm PLD SRO buffer layer deposited at 700–800°C in 50–100 mTorr of O_2 pressure. Subsequently, a YBCO film of 680 nm thickness was deposited on the SRO layer with an energy density of 1–2 J/cm^2 and frequency of 8 Hz at 700–800°C in 200–300 mTorr of O_2. The YBCO film was then annealed inside the chamber at 450°C in 1 atm O_2 for 90 min. As shown by the XRD pole figures in Figure 14, YBCO keeps exactly the same orientation with MgO which confirms a cube-on-cube epitaxial relationship among YBCO, SRO, and the MgO film. The c-axis of YBCO is tilted at the β=35.5° angle, the same value as that of the MgO template. Strong peaks are observed on YBCO pole figure of (005), (103), and (113) planes, respectively. These pole figure analyses indicate excellent biaxial alignment of YBCO deposited on ISD with SRO buffers.

YBCO-coated conductors fabricated with the ISD-MgO capped with SRO buffer layer exhibited a sharp transition with T_c = 90 K. Transport $J_c = 0.68\times10^6$ A/cm^2 and I_c > 44 A/cm were measured at 77 K in self-field. Figure 15 plotted the I-V curve measured over the entire 0.6-cm width for this YBCO-coated conductor sample deposited on an SRO-buffered ISD MgO substrate (α = 55°). The thickness of this YBCO thin film is 0.68 μm.

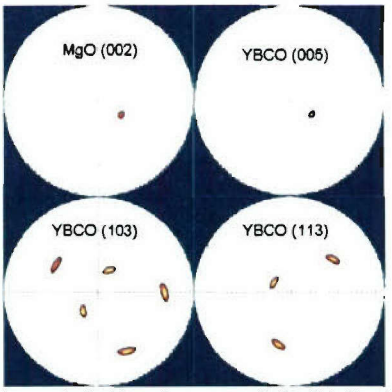

Figure 14. Pole figure analysis on MgO (002), YBCO (005), (103), and (113), respectively.

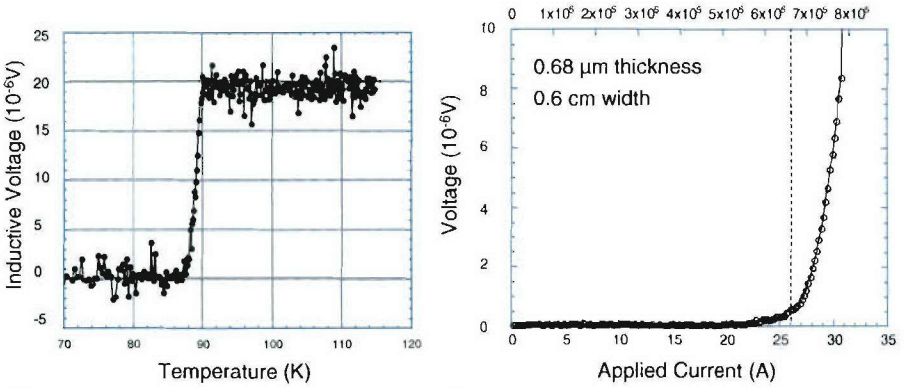

Figure 15. T_c and I_c measurement of the YBCO film deposited on ISD MgO with SRO cap layer.

Compared with the best result by the ISD MgO approach [25], the measured I_c and J_c in this experiment is still low. One of the concerns for the low J_c is the Ni diffusion which may degrade the YBCO performance. To investigate the possible Ni diffusion, a sample was prepared by following the similar processing conditions. SIMS analysis was performed on a 90x90 μm square region of this sample. Figure 16 is the chart of the SIMS analysis showing the depth profile of nickel and other elements. Ni is observed on the substrate part; however, its concentration decays rapidly through the barrier layer and ISD MgO layer to the background noise level. No Ni was observed in the SRO and YBCO layer. The other elements of HC have also been profiled. Again no diffusion has been detected.

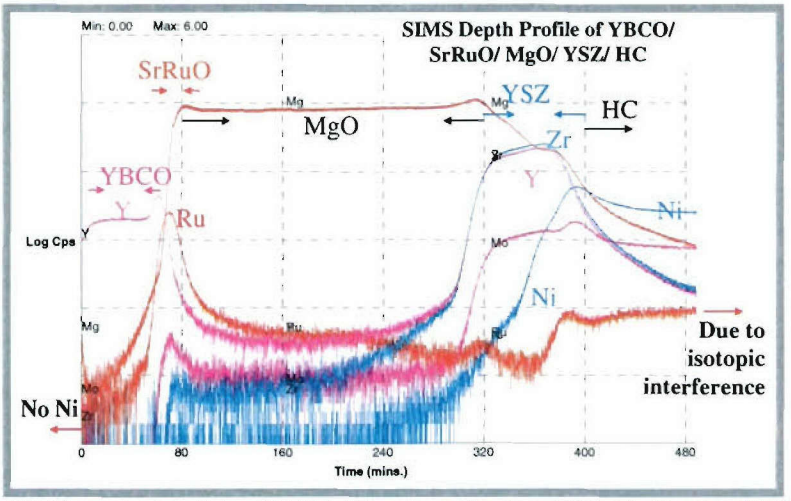

Figure 16. SIMS analysis of the YBCO film deposited on ISD MgO with SRO cap layer.

Surface roughness has long been known as a big factor of degradation of YBCO coated conductor, in particular in the ISD based YBCO coated conductor [30]. In our case, the approach of mechanical polishing of the long HC alloy tape could only remove large and deep scratches; however submicron features were still present. ISD MgO grown on rough substrate surface is rougher compared with those on well polished substrates. Figure 17 is the AFM analysis of the ISD MgO on the lightly polished HC tape and well polished small HC sample. Table 2 shows the AFM surface statistics derived from the AFM analysis. These data reveal that the roughness of ISD MgO (23.66 nm) on long HC tape is more than double than that on highly polished small sample (11.16 nm). Thus, low J_c of YBCO on ISD MgO grown on lightly polished HC alloy tape could be partly due to the roughness of the substrate. This is evident from comparison of a 0.68 μm YBCO grown at ANL on a highly polished HC sample with ISD MgO and SRO cap layers. I_c measurement (Figure 18) shows that by using the highly polished HC surface, J_c increased from 0.68 MA/cm^2 to over 1.6 MA/cm^2, and I_c increased to 110 A/cm.

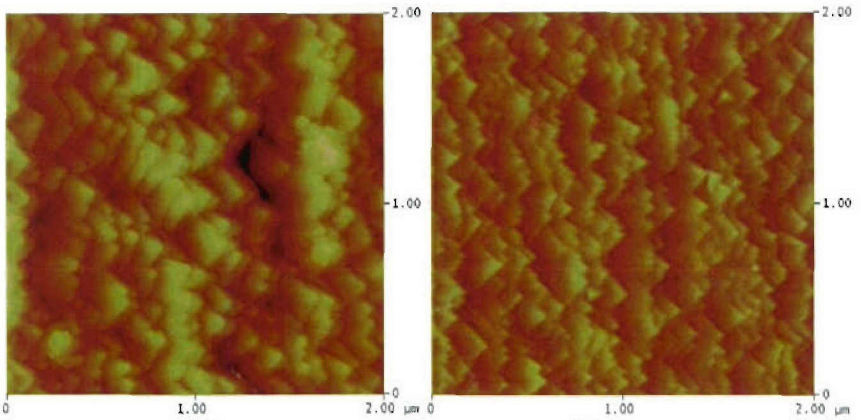

(a) (b)

Figure 17. AFM surface analysis of the ISD MgO template deposited on (a) lightly mechanical polished HC tape and (b) well polished small HC sample.

Table 2. AFM surface statistics of ISD MgO template deposited on lightly mechanical polished HC tape and well polished small HC sample

Image statistics	Lightly polished HC tape	Highly polished HC small sample
Img. Z range (nm)	232.14	94.54
Img. Rms (Rq, nm)	29.84	13.72
Img. Ra (nm)	23.66	11.16
Img. Srf. Area (μm^2)	5.62	4.76
Img. Srf. Area diff (%)	40.60	19.11

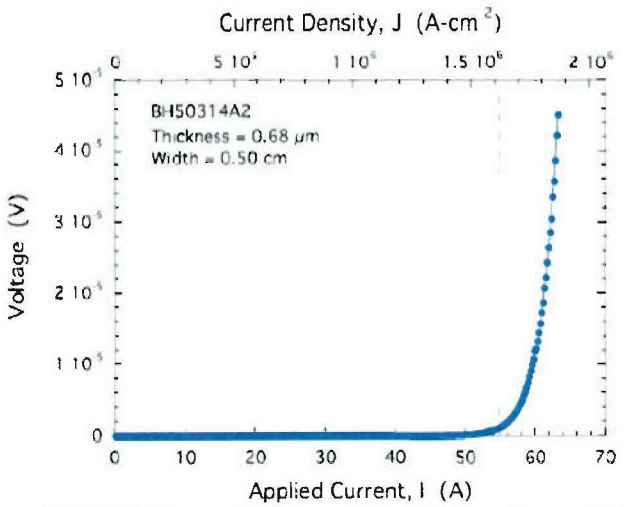

Figure 18. I_c measurement of YBCO film on highly polished HC surface with ISD MgO template and SRO buffer layers

4.5 MOD OF YBCO

High performance YBCO films have been demonstrated on RABiT substrates through a MOD approach at ORNL [31-34]. In order to develop and optimize the MOD process for ISD MgO substrate, a chemistry lab has been set up at UES.

The sol was made by hybrid fluorine-free precursor of TMAP yttrium and copper salts with barium trifluoacetate. The YBCO films with thickness of 0.65 μm were made by the traditional MOD approach including spin coating, pyrolysis (burnout), and conversion (anneal). Texture characterizations of films deposited on ORNL's RABiT substrates performed in XRD four-circle diffractometer confirmed that the volume fraction of cubic phase (termed as c-axis oriented Y123 phase with in plane texture) was over 95%. Both un-bridged and bridged samples had carried high current density over 2.2 MA/cm^2. The critical transition temperature measurement showed zero resistance temperature over 92K. All the data in Jc, Tc, and texture measurements show high quality reproducible YBCO films by this MOD approach.

Initial deposition of MOD YBCO on ISD MgO substrates have been carried out. A small percentage of YBCO on ISD substrate has been found to be textured by using the same solution and process conditions that produce good films on RABiT substrates. Thus, more optimization of the MOD process parameters is needed for ISD substrates.

5.0 SUMMARY

Long length highly textured MgO template has been successfully deposited on HC substrate in the reel-to-reel system. High deposition rate up to 10 nm/sec of the ISD MgO ebeam deposition and broad exposure window of 7 cm have been achieved with the average in-plane texture of FWHM=10°. With this set up the output of the well textured MgO template can be easily reached to 1 m/hr. Texture formation of the MgO layer has been investigated by XRD analysis. A new relationship termed "two-third relationship"between inclined angle and the tilted angle of (001) plane is found for the present experimental set up. Microstructure and Surface morphology investigations show that the requirement of reducing surface energy while maintaining the [11n] preferred growth direction has truncated MgO columnar growth with {100} faces, one of which is rotated to face the vapor direction to result in the highest capture cross section. This is the foundation of the principle of in-plane texture formation in the oblique or ISD deposition. No Ni diffusion to the YBCO film has been determined. It is conjectured that the lower J_c and I_c resulted from the rough surface of the HC tape. High performance tape with J_c>1.6 MA/cm^2 and I_c>110 A/cm have been demonstrated on well polished HC small samples. A chemistry lab has been setup for MOD YBCO deposition at UES. Initial deposition of MOD YBCO on ISD MgO substrates have been carried out. Results indicate that more optimization of the MOD process parameters is needed for ISD substrates.

REFERENCES

1. Larbalestier, D., et al., *High-T_c superconducting materials for electric power applications.* Nature, 2001. **414**(6861): p. 368-377.
2. Wu, X.D., et al., *Properties of $YBa_2Cu_3O_{7-Delta}$ Thick-Films on Flexible Buffered Metallic Substrates.* Applied Physics Letters, 1995. **67**(16): p. 2397-2399.
3. Iijima, Y., et al., *Biaxial alignment control of $YBa_2Cu_3O_{7-x}$ films on random Ni- based alloy with textured yttrium stabilized-zirconia films formed by ion-beam-assisted deposition.* Journal of Materials Research, 1997. **12**(11): p. 2913-2923.
4. Dimos, D., P. Chaudhari, and J. Mannhart, *Superconducting Transport-Properties of Grain-Boundaries in Yba2cu3o7 Bicrystals.* Physical Review B, 1990. **41**(7): p. 4038-4049.
5. Knierim, A., et al., *High critical current densities of YBa2Cu3O7-x thin films on buffered technical substrates.* Applied Physics Letters, 1997. **70**(5): p. 661-663.
6. Dimos, D., et al., *Orientation Dependence of Grain-Boundary Critical Currents in $YBa_2Cu_3O_{7-Delta}$ Bicrystals.* Physical Review Letters, 1988. **61**(2): p. 219-222.
7. Goyal, A., et al., *High critical current density superconducting tapes by epitaxial deposition of $YBa_2Cu_3O_x$ thick films on biaxially textured metals.* Applied Physics Letters, 1996. **69**(12): p. 1795-1797.

8. Norton, D.P., et al., *Epitaxial $YBa_2Cu_3O_7$ on biaxially textured nickel (001): An approach to superconducting tapes with high critical current density.* Science, 1996. **274**(5288): p. 755-757.
9. Iijima, Y., et al., *Processing and transport characteristics of YBCO tape conductors formed by IBAD method.* Applied Superconductivity, 1996. **4**(10-11): p. 475-485.
10. Iijima, Y., et al., *Biaxially Aligned $YBa_2Cu_3O_{7-X}$ Thin-Film Tapes.* Physica C, 1991. **185**: p. 1959-1960.
11. Wu, X.D., et al., *High-Current Yba2cu3o7-Delta Thick-Films on Flexible Nickel Substrates with Textured Buffer Layers.* Applied Physics Letters, 1994. **65**(15): p. 1961-1963.
12. Foltyn, S.R., et al., *High-T_c coated conductors - Performance of meter-long YBCO/IBAD flexible tapes.* IEEE Transactions on Applied Superconductivity, 1999. **9**(2): p. 1519-1522.
13. Hasegawa, K., et al., *Biaxially aligned YBCO film tapes fabricated by all pulsed laser deposition.* Applied Superconductivity, 1996. **4**(10-11): p. 487-493.
14. Bauer, M., R. Semerad, and H. Kinder, *YBCO films on metal substrates with biaxially aligned MgO buffer layers.* IEEE Transactions on Applied Superconductivity, 1999. **9**(2): p. 1502-1505.
15. Balachandran, U., et al., *Inclined-substrate deposition of biaxially textured template for coated conductors.* Physica C-Superconductivity and Its Applications, 2002. **378**: p. 950-954.
16. Harper, J.M.E., et al., eds. Ion Bombardment Modification of surfaces, ed. A. and and R. Kelly. 1984, Elsevier: New York.
17. Rossnagel, S.M. and J.J. Cuomo, MRS Bull, 1987. **12**: p. 40.
18. Prusseit, W., et al. *Continuous coated conductor fabrication by evaporation.* in *Mat. Res. Soc. Symp.* 2004.
19. Sugano, M., et al., *Intrinsic strain effect on critical current and its reversibility for YBCO coated conductors with different buffer layers.* SUPERCONDUCTOR SCIENCE & TECHNOLOGY, 2005. **18**(3): p. 369-372.
20. Ma, B., et al., *High critical current density of YBCO coated conductors fabricated by inclined substrate deposition.* Physica C, 2004. **403**: p. 183-190.
21. Smith, D.O., *Anisotropy in permalloy films.* J. Appl. Phys., 1959. **30**(4): p. 264S-265S.
22. Smith, D.L., *Thin-Film Deposition Principle and Practice*, ed. D.L. Smith. 1995, New York: McGraw-Hill, Inc.
23. Abelmann, L. and C. Lodder, *Oblique evaporation and surface diffusion.* Thin Solid Films, 1997. **305**(1-2): p. 1-21.
24. Smith, D.O., M.S. Cohen, and G.P. Weiss, *Oblique-incidence anisotropy in evaporated permalloy films.* J. Appl. Phys., 1960. **30**(10): p. 1755-1762.
25. Prusseit, W., et al., *Commercial coated conductor fabrication based on inclined substrate deposition.* IEEE Transactions on Applied Superconductivity, 2005. **15**(2): p. 2608-2610.
26. Balachandran, B., B. Ma, and D.J. Miller. *Development of coated conductor by inclined substrated deposition.* in *2004 Annual Peer Review.* 2004. Washington DC.
27. Uprety, K.K., et al., *Growth and properties of YBCO-coated conductors on biaxially textured MgO films prepared by inclined substrate deposition.* Superconductor Science & Technology, 2005. **18**(3): p. 294-298.
28. Nieuwenhuizen, J.M. and H.B. Haanstra, Philips Tech. Rev., 1966. **27**: p. 87.
29. Paritosh and D.J. Srolovitz, *Shadowing effects on the microstructure of obliquely deposited films.* Journal of Applied Physics, 2002. **91**(4): p. 1963-1972.
30. Koritala, R.E., et al., *Surface roughness of magnesium oxide buffer layers grown by inclined substrate deposition.* IEEE Transactions on Applied Superconductivity, 2005. **15**(2): p.3031-3033.
31. Xu, Y., et al., *Fabrication of High J_c $YBa_2Cu_3O_{7-d}$ Films Using A Fluorine-Free Sol Gel Approach.* J. Mater. Res., 2003. **18**(3): p. 677-681.
32. Xu, Y., et al., *High performance YBCO films by the hybrid of non-fluorine yttrium and copper salts with Ba-TFA.* Physica C, 2005. **421**: p. 67-72.

33. Xu, Y., et al., *Liquid Phase Enhanced Hybrid MOD Approach for High Performance YBCO Films Development.* IEEE Transactions on Applied Superconductivity, 2005. **15**(2): p. 2617-2619.
34. Xu, Y., et al., *Preparation of YBCO Films on CeO_2-Buffered (001) YSZ Substrates by a Non-Fluorine MOD Method.* J. of Am. Ceram. Soc., 2004. **87**(9): p. 1669-1676.